ΜΕΘΟΔΟΙ ΑΞΙΟΛΟΓΗΣΗΣ ΟΣΤΙΚΗΣ ΑΡΧΙΤΕΚΤΟΝΙΚΗΣ

Ιωάννης Π. Σταθόπουλος, MD, MSc

Ορθοπαιδικός Χειρουργός

Bone 116 (2018) 215–220

Contents lists available at ScienceDirect

Bone

journal homepage: www.elsevier.com/locate/bone

Full Length Article

The trabecular bone score: Relationships with trabecular and cortical microarchitecture measured by HR-pQCT and histomorphometry in patients with chronic kidney disease

J. Ramalho[a], I.D.B. Marques[a], Didier Hans[b], David Dempster[c,d], Hua Zhou[d], Parth Patel[e], R.M.R. Pereira[f], V. Jorgetti[a,g], R.M.A. Moyses[a,h], Thomas L. Nickolas[i,*]

- TBS has not been validated as a measure of trabecular architecture against transiliac bone biopsy with histomorphometry in CKD patients
- We hypothesized that TBS would reflect trabecular architecture at the iliac crest in CKD patients
- tetracycline double labeled transiliac crest bone biopsy, areal BMD of the spine, total hip, femoral neck (FN) and spine TBS by DXA, and cortical and trabecular volumetric density and microarchitecture by HR-pQCT

Table 2
Spearman correlations between TBS and HR-pQCT/histomorphometric parameters.

Parameter	rho value	p value
N = 50		
Radius HR-pQCT parameters		
Total volumetric BMD	0.41	0.004
Trabecular volumetric BMD	0.52	< 0.001
Cortical volumetric BMD	0.17	0.2
BV/TV	0.42	0.003
TbN	0.27	0.06
TbTh	0.41	0.003
TbSp	−0.33	0.02
CtTh	0.16	0.3
Tibia HR-pQCT parameters		
Total volumetric BMD	0.33	0.02
Trabecular volumetric BMD	0.25	0.1
Cortical volumetric BMD	0.50	< 0.001
BV/TV	0.25	0.1
TbN	0.07	0.7
TbTh	0.19	0.2
TbSp	−0.09	0.6
CtTh	0.40	0.005
Histomorphometric parameters		
BV/TV	0.65	< 0.001
Tb.Wi	0.61	< 0.001
Tb.N	0.23	0.1
Tb.Sp	−0.38	0.006
Ct.Wi	−0.35	0.01
Ct.Po	−0.02	0.9
BFR/BS	0.15	0.3
MS/BS	0.20	0.2
MAR	0.27	0.1
Mlt	0.01	0.9

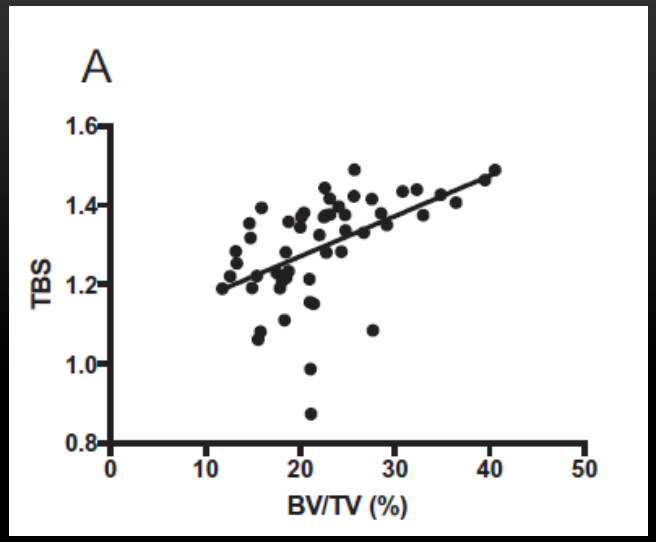

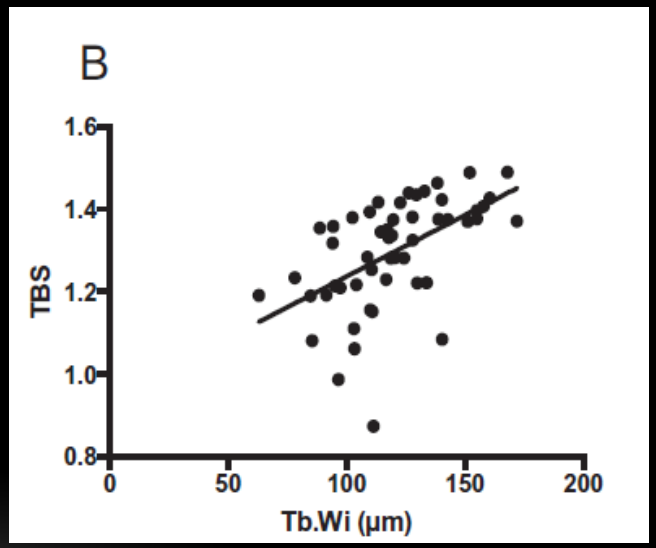

Table 3

Univariate linear regression for relationships between 2D histomorphometric measures and TBS, DXA and anthropomorphic characteristics.

	Regression coefficient (95% Confidence Interval)	p value
N = 50		
BV/TV		
TBS	37.29 (23.0–51.59)	< 0.001
FN *Z*-score	2.57 (0.47–4.67)	0.02
Height (cm)	0.26 (0.07–0.46)	0.01
Weight (kg)	0.14 (−0.01–0.26)	0.03
Tb.Wi		
TBS	124.04 (72.66–175.43)	< 0.001
FN Z-score	9.26 (1.94–16.58)	0.01
Height (cm)	1.05 (0.39–1.71)	0.002
Weight (kg)	0.36 (−0.08–0.79)	0.1
Tb.Sp		
TBS	−573.17 (−1001.63 to −144.72)	0.01
FN Z-score	−5.07 (−62.20–52.05)	0.9
Height (cm)	−1.14 (−6.45–4.16)	0.7
Weight (kg)	−1.11 (−4.37–2.16)	0.5
Ct.Wi		
TBS	−0.72 (−1.34 to −0.10)	0.02
FN Z-score	0.06 (−0.02–0.14)	0.1
Height (cm)	−0.001 (−0.01–0.01)	0.8
Weight (kg)	−0.001 (−0.004–0.01)	0.7

BV/TV trabecular bone volume, TBS trabecular bone score, FN femoral neck, Tb.Wi trabecular width, Tb.Sp trabecular separation, Ct.Wi trabecular width.

Table 4
Multivariate analysis for relationships between 2D histomorphometric measures and TBS, DXA and anthropomorphic characteristics.

	B	B CI 95%		p value
N = 50				
BV/TV				
TBS	45.57	26.9	60.25	< 0.001
Weight (kg)	0.17	0.04	0.31	0.01
Height (cm)	−0.16	−0.38	0.06	0.2
FN Z-score	0.72	−1.21	2.66	0.5
Tb.Wi				
TBS	109.49	48.54	170.44	0.001
Height (cm)	3.37	0.19	6.56	0.04
Weight (kg)	9.10	0.82	17.37	0.03
Weight × height	−0.05	−0.10	−0.004	0.04
FN Z-score	4.15	−2.92	11.22	0.2

BV/TV trabecular bone volume, TBS trabecular bone, FN femoral neck, Tb.Wi trabecular width.

In conclusion, our data suggest that TBS, a novel and widely available tool to assess trabecular architecture, reflected trabecular micro-architecture and cortical width measured by bone histomorphometry in CKD patients. These data add to the growing body of literature on the use of TBS to assess skeletal health in CKD patients; future studies should address its application and utility in CKD patients, including thresholds that indicate highest risk of fracture and whether changes in TBS reflect changes in fracture incidence and responses to anti-fracture strategies.

Bone 123 (2019) 8–17

Contents lists available at ScienceDirect

Bone

journal homepage: www.elsevier.com/locate/bone

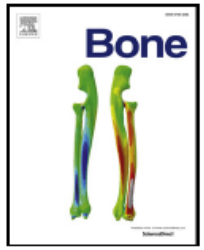

Full Length Article

Ultrashort echo time magnetic resonance imaging (UTE-MRI) of cortical bone correlates well with histomorphometric assessment of bone microstructure

Saeed Jerban[a,*], Yajun Ma[a], Jonathan H. Wong[b], Amin Nazaran[a], Adam Searleman[a], Lidi Wan[a], Judith Williams[b], Jiang Du[a], Eric Y. Chang[b,a,**]

[a] Department of Radiology, University of California, San Diego, CA, USA
[b] Radiology Service, VA San Diego Healthcare System, San Diego, CA, USA

- Porosity in cortical bone can determine bone mechanical properties and its fracture risk
- Although clinical MRI shows void signal for cortical bone, ultrashort echo time (UTE) MRI can image and quantitatively assess cortical bone

- Water in bone: a) bound to the collagen matrix (bound water) - indirect measure of the collagen matrix and b) free water in bone pores (pore water) represents the bone porosity
- Intracortical bone porosity includes a range of pore classes and sizes, including Haversian canals (10–200 μm), lacunae (1–10 μm), and canaliculi (0.1–1 μm)
- μCT can only measure a portion of large Haversian canals, practically adequate to accurately characterize pores larger than 40 μm in size (4 voxels approx.)

- This study investigated the correlations between UTE-MRI based quantifications and histomorphometric measures of bone porosity that cover all pores larger than 1 μm
- Anterior tibial midshaft specimens from eleven donors (51 ± 16 years old, 6 males, 5 females)
- clinical 3 T-MRI using UTE magnetization transfer (UTE-MT, three power levels and five frequency offsets) and UTE-T2* sequences
- μCT at 9 μm voxel size
- Histomorphometry

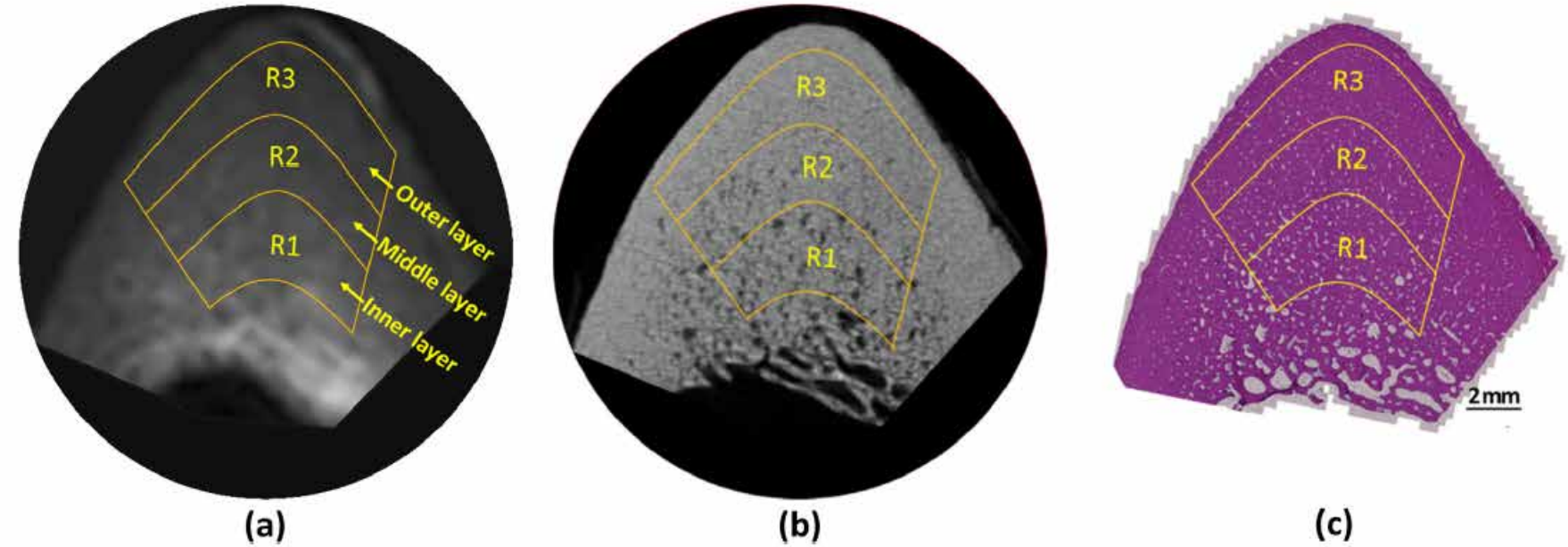

Fig. 1. Selected ROIs at three different bone layers on a representative bone specimen (Male, 71 years old) illustrated on (a) UTE-MRI (250 μm pixel size), (b) μCT (9 μm pixel size), and (c) histology (H&E stained, 0.2 μm pixel size) images.

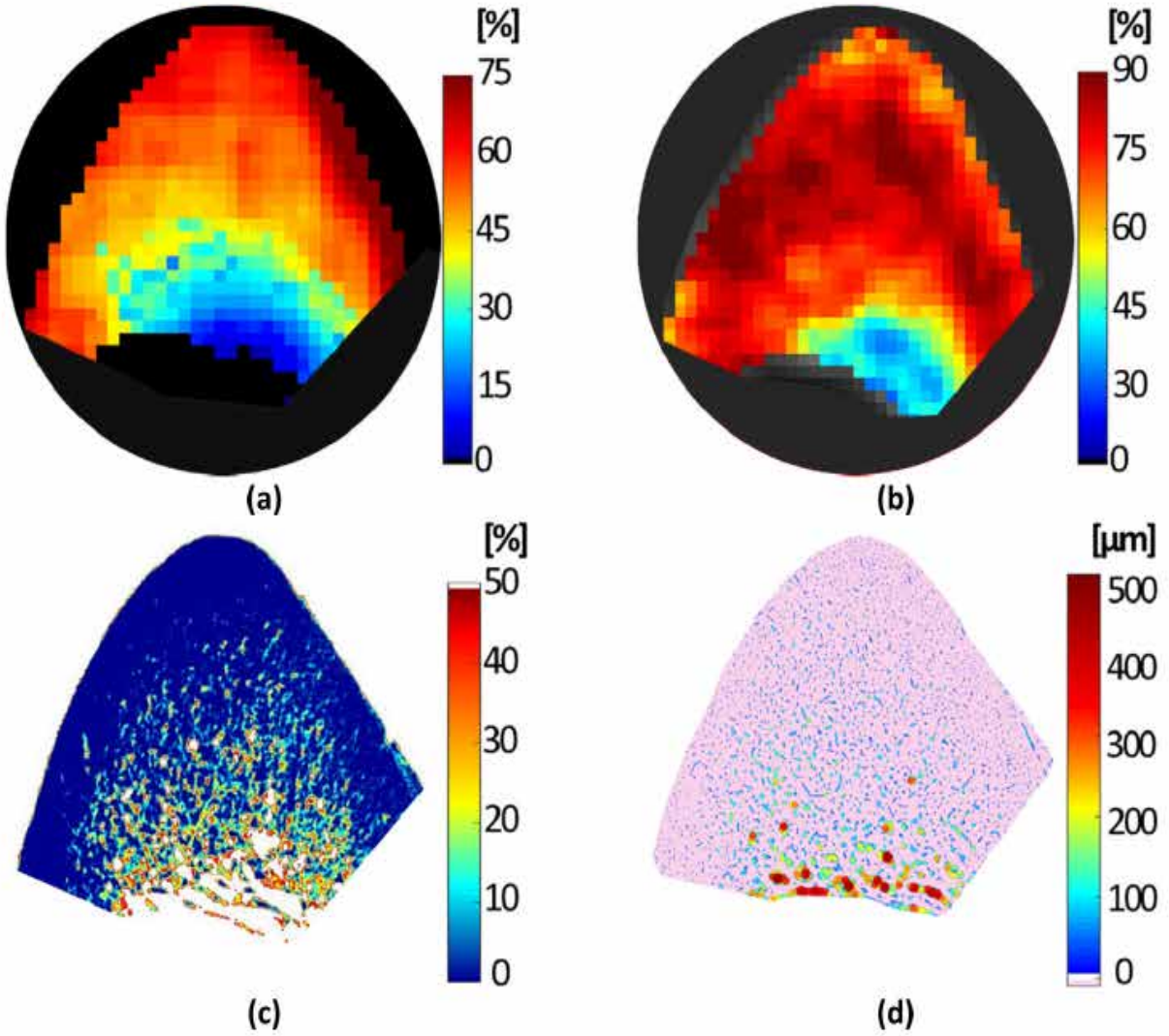

Fig. 4. (a) Macromolecular fraction (MMF) from MT modeling, (b) Frac1 (short-T2* component) from bi-component T2* fitting, (c) µCT-based porosity, and (d) histomorphometry-based pore size maps of a representative anterior tibial bone specimen (71-year-old male).

Table 2

Pearson's correlations, 95% intervals, and p values between microstructural measures (histomorphometric and μCT-based) and UTE-MRI parameters (bi-component T2* fitting and MT modeling). Significance for all correlations were assessed using non-parametric bootstrap (with resampling by specimen) to adjust for within-specimen dependence.

			Bi-component T2* fitting			MT-modeling	
			Frac1	$T2^*_1$	$T2^*_2$	MMF	$T2_{MM}$
μCT		Porosity	−0.71 [−0.89, −0.18] p < 0.01	−0.76 [−0.89, −0.51] p < 0.01	0.09 [−0.31,0.42] p = 0.74	−0.87 [−0.92, −0.77] p < 0.01	0.37 [−0.24,0.61] p = 0.18
		BMD	0.68 [0.17,0.83] p < 0.01	0.61 [0.45,0.75] p < 0.01	−0.06 [−0.29,0.31] p = 0.86	0.85 [0.70,0.91] p < 0.01	−0.25 [−0.68,0.43] p = 0.50
Histomorphometry	Porosity	All pores	−0.71 [−0.85, −0.45] p < 0.01	−0.71 [−0.83, −0.53] p < 0.01	0.11 [−0.31,0.44] p = 0.63	−0.81 [−0.89, −0.65] p < 0.01	0.61 [0.25,0.78] p < 0.01
		Small pores (< 40 μm)	−0.52 [−0.74, −0.23] p < 0.01	−0.42 [−0.81, −0.09] p = 0.02	0.02 [−0.26,0.39] p = 0.88	−0.56 [−0.77, −0.34] p < 0.01	0.26 [−0.22,0.76] p = 0.26
		Large pores (> 40 μm)	−0.69 [−0.83, −0.43] p < 0.01	−0.70 [−0.82, −0.53] p < 0.01	0.11 [−0.31,0.45] p = 0.62	−0.78 [−0.88, −0.64] p < 0.01	0.61 [0.29,0.78] p < 0.01
	Pore size	All pores	−0.55 [−0.74, −0.22] p < 0.01	−0.71 [−0.85, −0.53] p < 0.01	0.15 [−0.39,0.54] p = 0.58	−0.73 [−0.85, −0.55] p < 0.01	0.65 [0.41,0.81] p < 0.01
		Small pores (< 40 μm)	−0.60 [−0.80, −0.35] p < 0.01	−0.42 [−0.78,0.16] p = 0.17	−0.19 [−0.61,0.20] p = 0.37	−0.51 [−0.79, −0.21] p < 0.01	0.27 [−0.16,0.67] p = 0.23
		Large pores (> 40 μm)	−0.55 [−0.76, −0.21] p < 0.01	−0.70 [−0.86,0.52] p < 0.01	0.14 [−0.40,0.52] p = 0.61	−0.74 [−0.86, −0.54] p < 0.01	0.64 [0.39,0.80] p < 0.01

Two-pool MT modeling and bi-component T2* fitting techniques were investigated for their capability of cortical bone porosity assessment as measured through histomorphometric analyses performed on submicron resolution histology images. MMF from MT modeling as well as Frac1 and T2*1 from bi-component T2* fitting showed strong correlations with histomorphometric total and large-pores porosities as well as with μCT-based porosity. Remarkably, studied UTE-MRI techniques were able to detect small pores variations with moderate correlations. This study highlighted the capability of UTE-MRI techniques for detecting variation of bone porosity in the form of pores below the range detectable by μCT, including lacunae and small Haversian canals, which can contribute differently in bone disease, injury, and remodeling.

Bone 114 (2018) 206–214

Contents lists available at ScienceDirect

Bone

journal homepage: www.elsevier.com/locate/bone

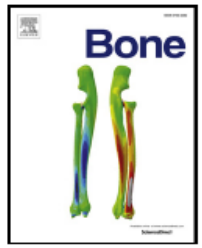

Full Length Article

Quantification of bone microstructure in the wrist using cone-beam computed tomography

Karen Mys[a,*], Filip Stockmans[b], Evie Vereecke[b], G. Harry van Lenthe[a]

[a] Biomechanics Section, Department of Mechanical engineering, KU Leuven, Leuven, Belgium
[b] Muscles & Movement, Department of development and Regeneration, KU Leuven Campus Kulak, Kortrijk, Belgium

- microCT is the gold standard in 3D imaging of trabecular bone structure (limited to ex vivo)
- HR-pQCT for bone microarchitecture in vivo (limited to scanning extremities, with a limited field of view and long scanning time (~2 - 3 min. for a stack of 0.9 cm)
- Cone-beam computed tomography (CBCT) is a promising alternative with a much larger field of view. Yet, CBCT is challenged by artefacts that reduce image contrast, such that it is currently being used for qualitative evaluation only.

- Therefore, the aims of this work were (1) to enhance image contrast and (2) to determine the accuracy of high-resolution CBCT for bone microarchitectural assessment.

- 19 trapezia (12 right, 7 left; 18 female, 1 male) were removed from the hands of arthritic patients ranging in age from 53 to 76 years (mean 63.4 years)
- microCT, SkyScan 1172, Bruker, Belgium) at a voxel size of 19.84 μm
- Cone-beam computed tomography (CBCT, NewTom 5G, Cefla, Italy) at 75 μm

- Bone morphometric parameters: bone volume (BV), total tissue volume (TV), bone volume fraction (BV/TV), bone surface density (BS/TV), trabecular thickness (Tb.Th), trabecular separation (Tb.Sp) and trabecular number (Tb.N)

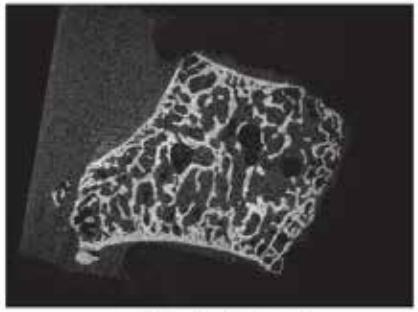

(a) *MicroCT (19.84μm)*

(b) *MicroCT segmented*

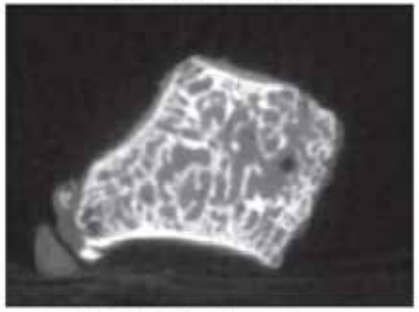

(c) *CBCT RManufacturer (75μm)*

(d) *CBCT RManufacturer segmented*

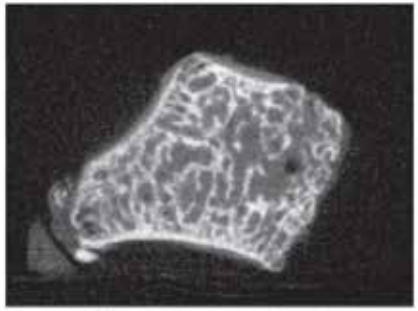

(e) *CBCT RInHouse (60μm)*

(f) *CBCT RInHouse segmented*

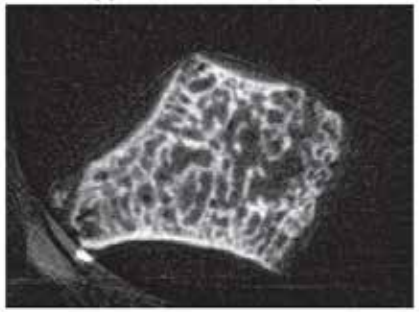

(g) *CBCT RInHouseBeam (60μm)*

(h) *CBCT RInHouseBeam segmented*

Table 2
Relative error (δe) with standard deviation and coefficients of determination between microCT and RManufacturer (standard scanner's reconstruction), RInHouse (in house reconstruction) and RInHouseBeam (in house reconstruction with beam hardening correction) for all samples ($N = 19$). RInHouseBeam outperformed RManufacturer and provided smaller bias as well as higher correlations.

		CBCT (N = 19)					
	MicroCT	RManufacturer		RInHouse		RInHouseBeam	
	Mean(SD)	$\delta\epsilon$(SD)	R^2	$\delta\epsilon$(SD)	R^2	$\delta\epsilon$(SD)	R^2
BV/TV [%]	23.38(2.8)	55.14(11.5)%	0.60	48.20(10.4)%	0.65	38.33(9.9)%	0.69
Tb.Th [mm]	0.18(0.02)	114.24(17.9)%	0.52	66.39(11.0)%	0.68	59.96(10.2)%	0.68
Tb.Sp [mm]	0.61(0.07)	9.43(5.7)%	0.84	−4.45(5.4)%	0.81	0.98(7.0)%	0.73
Tb.N [1/mm]	1.30(0.11)	−27.74(3.4)%	0.63	−10.91(3.3)%	0.82	−13.53(4.0)%	0.81
BS/TV [1/mm]	4.79(0.35)	−28.99(3.5)%	0.50	−9.7(4.0)%	0.72	−10.45(4.5)%	0.72

Significant correlations were found between the CBCT-based bone parameters and the microCT-based parameters with $R^2 > 0.68$ The in-house reconstructed software outperformed the commercial software. Smaller bias (overestimation of Tb.Th decreased from 114.24% to 59.96%) as well as higher correlations were observed for the in-house processed images. Still, a significant overestimation was observed for BV/TV and Tb. Th and an underestimation for Tb.N.

Original Article

Subchondral bone microarchitecture analysis in the proximal tibia at 7-T MRI

Agten, Christoph A; Honig, Stephen; Saha, Punam K; Regatte, Ravinder; Chang, Gregory (2018). Subchondral bone microarchitecture analysis in the proximal tibia at 7-T MRI. Acta Radiologica, 59(6):716-722.
DOI: https://doi.org/10.1177/0284185117732098

- Purpose: To compare subchondral bone microarchitecture parameters in the medial and lateral tibia plateau in individuals with and without fragility fractures

- Material and Methods: Twelve female patients (mean age 58±15 years; six with and six without previous fragility fractures) were examined with DXA and 7-T MRI of the proximal tibia.
- Digital topological analysis (DTA) was applied
- apparent bone volume; trabecular thickness; profile-edge-density (trabecular bone erosion parameter); profile-interior-density (intact trabecular rods parameter); plate-to-rod ratio; and erosion index
- 7-T whole-body MRI scanner (Siemens Magnetom, Siemens Healthcare, Erlangen, Germany) using a birdcage transmit, 28-channel receive array coil (Quality Electrodynamics, Mayfield Village, OH, USA)
- A 3D fast low angle shot (FLASH) sequence was implemented in the transverse plane

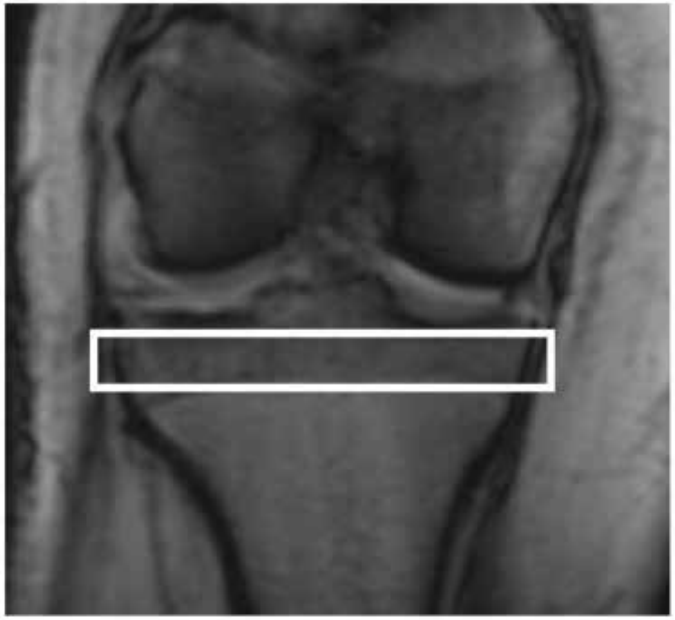

Fig. 1. Placement of volume of interest (white frame) in the subchondral bone of the proximal tibia on a coronal plane localizer MR image.

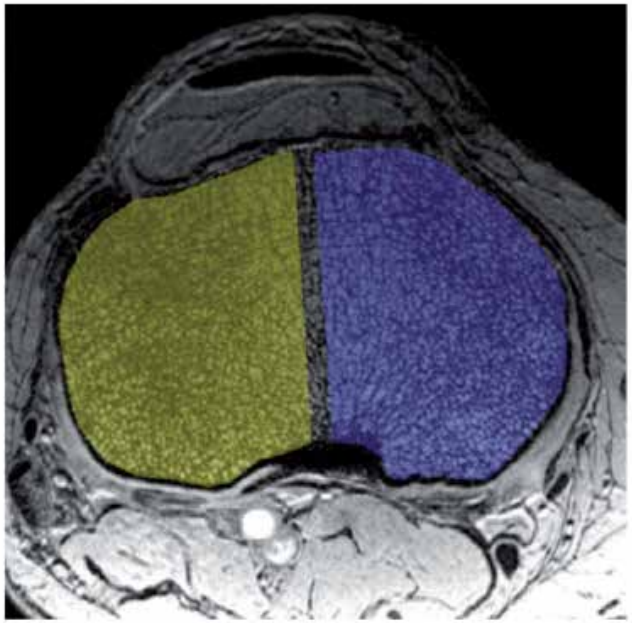

Fig. 2. Axial high-resolution MR images (7-T) through the epiphysis within the volume of interests in the proximal tibia. The medial (blue) and lateral (yellow) compartment are separated by a small safety margin. Digital topological analysis was performed in each compartment separately.

Table 1. Compartmental analysis.

	Medial					Lateral				
	Fracture cases		Controls			Fracture cases		Controls		
	Mean	SD	Mean	SD	*P* value	Mean	SD	Mean	SD	*P* value
ABV	0.295	0.022	0.317	0.009	0.016	0.296	0.019	0.314	0.011	0.078
Trabecular thickness (μm)	212.436	6.462	215.153	4.612	0.522	211.313	5.542	212.910	2.610	0.749
Profile edge density*	0.008	0.003	0.005	0.001	0.025	0.008	0.002	0.005	0.001	0.025
Profile interior density†	4.795	4.439	3.208	4.131	0.631	6.542	4.073	4.275	4.071	0.200
Plate-to-rod ratio	5.700	1.348	7.293	1.081	0.078	5.604	1.376	7.102	1.094	0.055
Erosion index	1.332	0.328	1.053	0.134	0.109	1.359	0.338	1.058	0.122	0.078

Results of digital topological analysis (DTA) within the subchondral bone of the tibia epiphysis in medial and lateral compartment.
*Trabecular bone erosion parameter.
†Parameter of intact trabecular rods.
ABV, apparent bone volume; SD, standard deviation.

In conclusion, 7-T MRI and DTA may permit detection of subtle regional deterioration in trabecular microarchitectural profile parameters when differences in BMD are not evident. The results suggest that this may serve as an early biomarker of osteoporosis and should be confirmed in larger prospective studies.

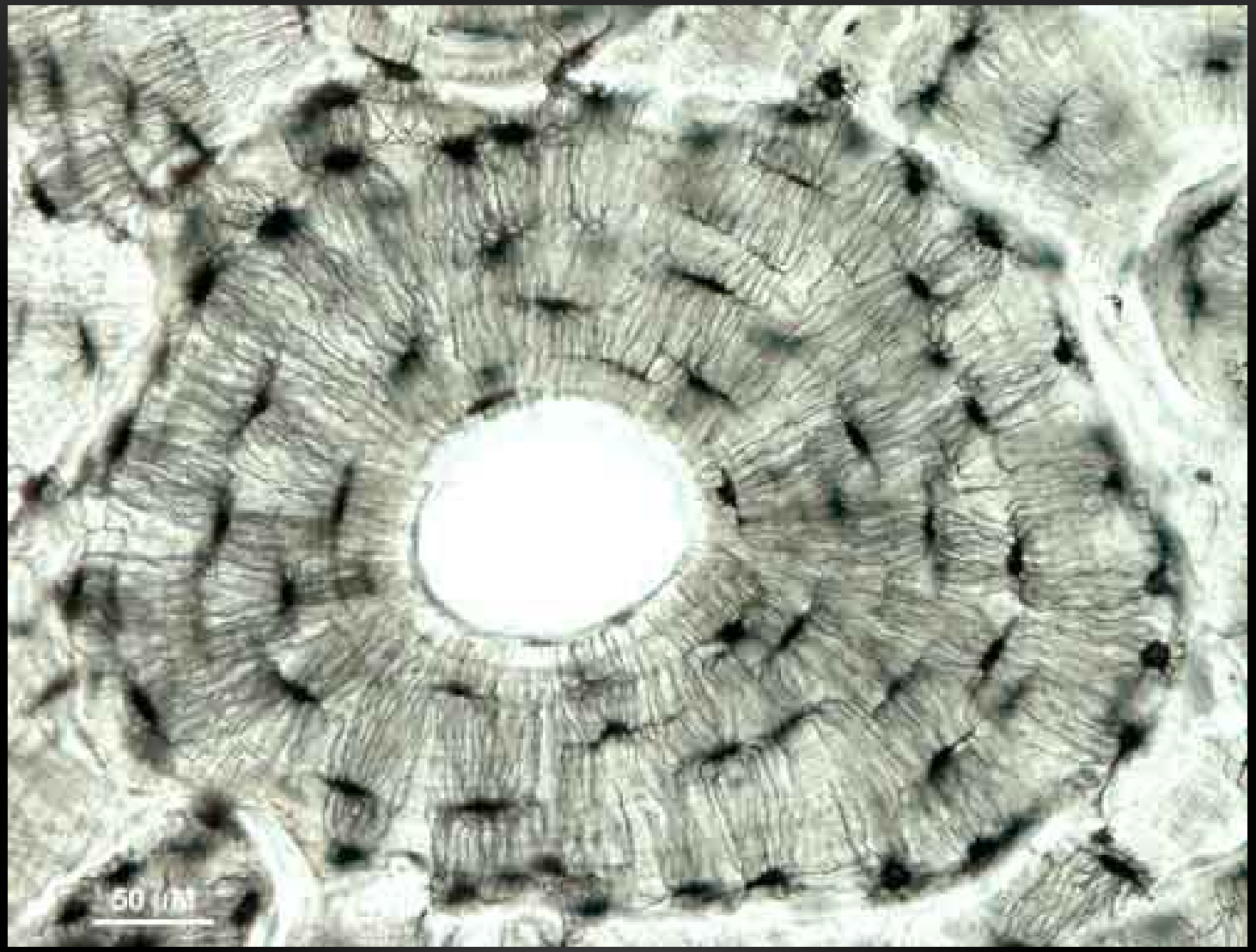

ΕΥΧΑΡΙΣΤΩ ΓΙΑ ΤΗΝ ΠΡΟΣΟΧΗ!!!